Frontal and Heat Content Variability in the Indian Sector of Southern Ocean during Austral Summer 2004

N. Anilkumar[+@], Alvarinho J. Luis[+], Y. K. Somayajulu[++], V. Ramesh Babu[++], M. K. Dash[+], K. N. Babu[+], M. Sudhakar[+], and P. C. Pandey[+]

[+]National Centre for Antarctic and Ocean Research, Headland Sada, Vasco-da-Gama, Goa 403804, INDIA.

[++]National Institute of Oceanography, Dona Paula, Goa 403004, INDIA.

Keywords: Oceanic fronts; Indian sector of Southern Ocean; Heat content; Mixed-layer thickness; Thermohaline structure; Winter Water; XBT/CTD.

@ Corresponding Author e-mail: anil@ncaor.org; anil3321@yahoo.com

Abstract

Two meridional CTD and XBT sections were covered along 45°E and 57°30'E to investigate the morphology of main fronts in the southwest Indian Ocean as a part of Indian pilot expedition to the Southern Ocean on board ORV Sagar Kanya. The frontal systems distinguish the different regimes of cold Antarctic waters from the warmer and saltier waters of the subtropical regime. Along 57°30'E, the signature of the Subtropical Front (STF) was a rapid decrease in surface temperature from 17°C to 10.6°C between 43°50'S and 45°40'S and it was identified as a broad frontal region with a southward shift compared to that at 45°E. The Subantarctic Front (SAF) and Polar Front (PF) were also located with remarkable features noted in the literature. PF was identified between 48° and 52°S along 45°E, where the surface temperature reduced from 5.5 to 2.7°C and where the northern limit of sub-surface temperature minimum layer (<2°C) is extended. This study reveals a southward shift of the oceanic fronts (STF and SAF) from west to east, with a maximum southward displacement of ~4° latitude for STF. The thermocline region was absent south of PF. An enhancement in the mixed layer thickness from 42° to 52°S occurred in association with the strengthening of the wind forcing. The presents of major watermasses like Subtropical Surface Water, Subantarctic Surface Water, Mode Water, Antarctic Intermediate Water, Circumpolar Deep Water and Antarctic Bottom Water were identified along the 45°E meridional section. Upper-ocean heat-content computation revealed a remarkable drop of 989 $\times 10^7$ J/m^2 (~42°S) and 1405 $\times$ 10^7 J/m^2 (~44°S) along 45° and 57°30'E, respectively. This sudden drop in heat content in turn affects the meridional heat transfer which is crucial for the studies related to global climatic variability.

1. Introduction

Hydrographic conditions in the Southern Ocean (SO) are modulated by an eastward flowing Antarctic Circumpolar Current (ACC) which is embedded with numerous circumpolar fronts (Nowlin and Klinck, 1986). SO is also a region of intense eddy activity that play an important role in both momentum and buoyancy fluxes which influence the global thermohaline circulation that affect the global climate (Huges and Ash, 2001). Earlier studies on changes in ACC transport were carried out in the central and eastern parts of Indian Ocean sector of the SO (Xiaojun et al., 2004; Sokolov and Rintoul, 2002; Rintoul and Sokolov, 2001; Rintoul et al., 1997; Rintoul et al., 2002, Rintoul and Bullister, 1999). However, its western part assumes greater significance as it receives heat largely through warm western boundary currents. This warm water gets trapped within the Agulhas retroflection and it exchanges heat with the atmosphere; this is the largest air-sea exchange in SO (Gordon, 2003).

There have been few studies on different oceanographic aspects of the eastern part of the southern sector of the Indian Ocean (Fu, 1986; Nagata et al, 1988; Park et al, 1993; Orsi et al., 1995; Belkin and Gordon, 1996; Sparrow et al., 1996; Holliday and Read, 1998; Park et al., 1998; Reid, 2003) which emphasized that the areas west of the Crozet Plateau and east of the Kerguelen - Amsterdam passage are the key regions where the fronts confluence and split again. Hence, the aforementioned researches in the South Indian/ SO focused on the vivid changes in the morphology of the fronts. While most of the above researches were based on sparse hydrographic observations, the present investigation employ XBT data sampled at a high spatial resolution (20~30 nautical miles) to identify, delineate and compare frontal characteristics in the upper ocean between two meridional sections along 45°E and 57°30'E. CTD observations made at 1° latitude have also been augmented to interpret the salinity structure along 45°E.

2. Material and Methods

The National Centre for Antarctic and Ocean Research (NCAOR), Goa organized a Pilot Expedition to the ice-free areas of the SO onboard ORV Sagar Kanya during austral

summer 2004 (January - February). This pilot expedition, as a prelude to the long-term observational programs in the SO, was a multi-disciplinary and multi-institutional in nature involving different Indian research organizations. XBT and CTD observations were taken from 31°S to 56°S along 45°E, while along 57°30'E only XBT observations were made from 48°S to 26°S due to bad weather. The locations of these observations are shown in Fig. 1.

The vertical temperature profiles were obtained using XBT probes (type:T-7; temperature accuracy: $\pm$0.15°C; depth resolution: 0.65m. The sea surface temperature (SST) was recorded using a bucket thermometer (accuracy: $\pm$0.1°C). A CTD [make: SBE 9/11, Sea-Bird Electronics, USA; accuracy- temperature: $\pm$0.001°C, conductivity: $\pm$0.0001S/m and depth $\pm$0.005% of the full scale) was lowered at selected station locations along 45°E. Additionally, we estimated salinity of in-situ samples collected at selected depths with Rosette sampler attached with the CTD by using an onboard salinometer [Autosal 8400A, Guildline, Canada], and necessary corrections were applied to CTD salinity.

XBT probes were launched at every 1° latitude interval and the data were recorded at every 0.65*m* depth interval. The density of XBT observations was increased to 20~30 nautical miles interval in the frontal regions, where the variations in SST were found to be more than 5°C within an interval of 1° latitude. CTD data along 45°E were used at every 1*m* depth interval up to 760*m* for plotting the salinity structure.

XBT profiles were quality controlled by following the guidelines in the CSIRO Cookbook (CSIRO, 1993). Based on the findings of Thadathil et al. (2002) and Ridgway (1995), we found that depth corrections were marginal to the XBT profiles.

Oceanic fronts were identified by using the characteristic property indicators. Since it is not easy to classify each front based on exact change in its characteristic parameters, the criteria adopted by elsewhere were considered (Peterson and Whitworth, 1989; Orsi et al., 1993; Read and Pollard,1993; Orsi et al.,1995; Belkin and Gordon, 1996; Sparrow

et al., 1996; Holliday and Read, 1998). The adopted property indicators for identification of fronts are given in Table 1.

Heat content of the upper ocean along 45°E and 57°30'E was estimated. The heat content of 0-500 *m* water column was computed along the two meridians since the horizontal extent of front rather than its vertical extent determines the heat storage. The heat content was estimated by using

$$H = \rho Cp\left[\int_{0}^{500} \overline{T} dz\right], \qquad (1)$$

where H is the heat content (J/m^2), ρ is the seawater density (kg/m^3) and C_p is the specific heat of seawater at constant pressure ($J/kg/°C$). The value for ρC_p is assumed as a constant (0.409×10^7 $J/m^3/°C$) and $\overline{T}$ is the depth-averaged temperature computed following Bathen (1971).

3. Results and Discussion

3.1 Frontal variability

The variations in the positions of the oceanic fronts along 45 and 57°30'E were delineated following the literature guidance (Table -1). Fig. 2a and 2b depict thermal structure along 45°E and 57°30'E prepared from the XBT data which was obtained during 29 January~17 February and 22~29 February, respectively. The vertical salinity structure prepared from CTD data along 45°E and 57°30'E is portrayed in Fig. 3a and 3b, respectively. At 45°E, the Subtropical Front (STF) and the Agulhas Return Front (ARF) were identified as a merged front between 40°15' and 42°15'S (Fig. 2a), as inferred by Sparrow et al. (1996). On the other hand, its position at 57°30'E was found to be between 43°50' and 45°40'S (Fig. 2b). Moving southwards the Subantarctic Front (SAF) was located between 43° and 47°E, while the Polar Front (PF) was identified between 48 and 52°E. At 57°30'E the SAF was delineated between 46 and 48°S. However the position of PF could not be demarcated due to lack of data south of 48°S.

Along both the meridional sections, a drop in surface temperature across STF/ARF (merged front following Belkin and Gordon, 1996; Sparrow et al., 1996) was about 8°C (Fig. 2a and 2b). Along 45°E, STF/ARF was characterized with a salinity gradient of 1.12‰ across 2° (Fig. 3a). STF is normally viewed as a boundary separating the subtropical surface waters and the subantarctic surface waters of ACC (Deacon, 1937). STF was also described as a broad frontal zone (STFZ) (Lutjeharms and Valentine, 1984). It is pertinent to note that Holliday and Read (1998) identified STF between 40 and 42°S along 55°E, compared to the present observation. ARF could not be distinguished as a separate front in the present investigation, as the study area is far away from the retroflection region.

A similar southward shift in the latitudinal position of SAF was also observed between the two meridional sections. At 45°E SAF was observed between 43° and 47°S (Figs. 2a and 3a) whereas it was encountered between 46°30' and 48°S along 57°30'E (Fig. 2b). Some remarkable differences compared to previous studies (Park et al, 1993; Belkin and Gordon, 1996; Sparrow et al., 1996) are noted in the position of SAF in the present study. SAF narrowed from ~4° to 1.5° latitude width along 45°E and 57°30'E sections, respectively. On the other hand, Holliday and Read (1998) reported a width of ~1.5° latitude along 45°E which is narrower than the present result. However, its width along 57°30'E exhibited small variations compared to that reported in the literature. We note that Lutjeharms and Valentine (1984) reported the width of SAF to be ~2.5° latitude, which deviates from our findings for both the meridional sections (Figs. 2a, 2b and 3a).

The PF was identified along 45°E between 48° and 52°S, where the surface temperature decreased from 5.5 to 2.7°C and at the northern limit of 2°C isotherm below 200 m (Fig. 2a). The PF was not noticeable along 57°30'E, since the observations were restricted upto 48°S. The signature of PF identified in the present study is comparable to the criteria adopted for its identification elsewhere (Fu, 1986; Nagata et al, 1988; Park et al, 1993; Orsi et al., 1995; Belkin and Gordon, 1996; Sparrow et al., 1996; Holliday and Read, 1998; Park et al., 1998; Reid, 2003). The changes in surface temperature across the PF (5.5 ~ 2.7°C) differed marginally compared to that reported in the previous studies

(Lutjeharms and Valentine, 1984; Sparrow et al., 1996; Holliday and Read, 1998). On the other hand, Menon et al. (1988) identified different fronts along 45°E between 43° and 60°S however, they did not report the STF and SAF; but the position of PF reported by them agrees with the present investigation.

3.2 Mixed Layer and Winter Water properties

Typical XBT profiles highlighting the mixed layer and thermocline variation between 31 and 56°S are presented in Fig. 4. The thermocline thickness extends from 40 to 150 *m* in the subtropical waters (31-39°S, Fig. 4a) however, its depth is reduced from 60 to100 *m* as it approaches the STF between 41 and 43°S (Fig. 4b). Between the subantartic to polar waters (from 45 to 55°S), the thermocline region was fully obliterated, and the minimum temperature observed in the subsurface layer (100-250 *m*) is the remnant of the previous years Winter Water (WW) (Fig. 4c).

The MLT is considered as the thickness of the top layer where the potential density changed by $0.02\sigma_\theta$ from the surface value Park et al. (1998). Fig. 5a, 5b, 6a and 6b portray the meridional variation of MLT, wind speed and Winter Water properties respectively, together with a polynomial fit to the data. The wind data was recorded at the bridge level (25 *m*) and has been corrected for ship's speed and heading. From 31 to 39°S, (Fig. 5) the thickness of mixed layer was less (varies from 10*m* to 58*m*) and thereafter it has increased predominantly up to 52°S (104*m*). On the other hand, wind speed exhibits a bimodal pattern with peaks at 34 and 49°S (Fig. 5b). Strong winds (>12 *m*/*s*) were observed in the subantarctic and Antarctic waters of the study area, where maximum thickness of MLT is evident. In general, Fig. 5 highlights that an increase in MLT is strongly associated with an increase in wind speed. However, between 52 and 56°S, the MLT showed a decreasing trend which correlates with the decreasing wind speed. In brief, our study reveals a rapid increase in MLT in the subantarctic waters (45 to 52°S), rather than in the subtropical and Antarctic waters, in association with the strengthening of the winds. Park et al. (1998) reported that the mixed layer thickness along 62°E varies between 120*m* to 35*m* from 55°S to Antarctic convergence whereas, it

was significantly less along 30°E .While comparing the thickness difference of MLT between the present and earlier studies (Park et al., 1998) it can be stated that the mixed layer thickness is closely correlated with the wind speed.

The Winter water depth was maximum at PF region (>160m) and decreased sharply to a minimum (120*m*) at 56°S (Fig. 6a). Nevertheless, in previous studies it was observed with a higher depth of 200*m* at the PF region and a lower depth varying between 45*m* at 30°E and 60*m* at 62 °E (Park et al., 1998). A strong and predominant correlation between the MLT, WW depth and wind speed was noticed from 49° to 56°S which reveals the influence of wind speed on mixing and variation of WW depth in the upper layers . The WW temperature showed a gradual decrease from north to south in the polar region, whereas a marginal augment at 54°S disclose the correlation with wind speed and MLT (Fig.6b).

3.3 North-south spreading of water masses

The water masses identified along the 45°E longitude based on the TS criteria are:
Surface water masses: Subtropical Surface Water (STSW is characterized by relatively high temperature and salinity (> 12°C and >35.1‰). In the present investigation the signatures of STSW was identified from 37 to 40°S, where surface temperature did not disclose much variation nonetheless, the salinity exhibited a difference of 0.3‰ (Fig 7-9, 10a and 10b). Subantarctic surface water (SASW) always found near the southern boundary of the frontal zone. It is characterized by the lower temperature and salinity (9°C, < 34.0) (Park et al. 1993). In this investigation it was found between 43° and 45°S (Fig 7-9, 11a and 11b). While nearing the PF region from the subtropics the surface water becomes colder and fresher (<5°C, <34‰) indicated the presents of Antarctic surface water (AASW). The AASW was obviously seen from 44° to 56°S in the present investigation (Fig 7-9, 12a and 12b). Just beneath the AASW the WW water was observed.

Mode water: North of the frontal zone, see the vertical structure of density (Fig.9), pycnostad was developed within the potential density anomaly range (26.5 to 26.8kg/m^3) and a depth range of 400 to 700*m*. This water mass is formed by deep winter convection in the area immediately north of the ACC, and appears in summer sections as a pycnostad (or thermostad) beneath the seasonal thermocline (Park et al., 1993; Stramma and Lutjeharms, 1997). This water mass was characterized by a wide range of property ($11<\theta<14$°C; $35.0<S<35.4$, $26.5 < \sigma_\theta < 26.7$ kg/m^3). These features of Mode Water found in this investigation are concatenated with the earlier investigations of winter hydrographic stations (McCartney, 1977; Park et al., 1991). The Mode water in the Crozet basin is not advected from the west but locally produced, winter overturning of the subtropical water of Agulhas origin in the western half of the basin will produce a water different from the one influenced by frontal mixing with subantarctic water in the eastern half of the Crozet Basin (Park et al., 1993). McCartney (1977, 1982) argued that all Mode Waters are associated with the circumpolar SAF, whereas Park et al. (1993) disagreed with his finding and stated that it is ambiguous at least in the Crozet Basin and they named the Mode Water as Subtropical Mode water. In the present investigation one of our significant findings is the identification of the cold and fresh Mode Water between 31° and 41°S (Fig 7-9, 10a, 10b and 11a), suggesting this water mass as a subtropical Mode Water.

Antarctic Intermediate Water (AAIW): The features of AAIW characterized by it's properties (temperature 4.4°C; salinity minimum 34.42; and σ_θ ~27.24 kg/m3) were identified north of the subtropical frontal zone, between 31° and 41°S (Fig 7-9, 10a, 10b and 11a). The depth of this water mass was identified between ~1150and ~1200*m*, which was reported earlier at 1100*m* (Blintoff and McDougall, 1999) and 1300*m* (Park et al., 1998). Molinelli(1981), Fine(1993), Toole and Warren(1993) reported that the region near the Kerguelen Plateau is a source of AAIW entering Indian Ocean and confined its presents in the Crozet Basin. Below the subantarctic Mode Water the Antarctic Intermediate Water (AAIW), indicated by a salinity minimum at about 1000*m* depth spreads northward to about 10°S (Stramma and Lutjeharms, 1997). In the western Indian Ocean an intensified circulation of AAIW was reported by Harris (1972) and this has been discussed by Toole and Warren (1993). However, in the present study a strong eddy

mixing between cold, fresh subantarctic water and warm, salty subtropical water was predominant, especially in the upper layers while crossing the frontal zone hence this water mass was identified at the subsurface layer immediately south of the frontal zone (Fig.7-9, 10a, 10b and 11a).

Circumpolar Deep Water (CDW): CDW was identified with it's remarkable feature (temperature ~2°C; salinity ~34.77‰; and σ_θ ~27.8 kg/m^3) in the study area. It occupies the depth range 2000-3800 *m* north of 45°S and it rises sharply to shallower depths south of the frontal zone. NADW with higher salinities (~34.8‰) transported from the South Atlantic to the southwestern corner of the Indian Ocean, is assumed to be obstructed strongly from distributing east of about 45°E by the Madagascar ridge (Toole and Warren, 1993). The properties of CDW near 45°E almost match with the properties of North Atlantic Deep Water (NADW) reported by Park et al. (1993).

Antarctic Bottom Water (AABW): Below the CDW the temperature and salinity were found to be decreasing which indicated the influence of AABW. In the present investigation AABW was demarcated from 49° to 56°S with a range of it's characteristic properties, temperature -0.165 to -0.62°C, salinity ~34.671 to 34.652‰ and σ_θ 27.848 to 27.856 kg/m^3 at 4100 to 4700*m* depth. It was reported that AABW enters the Madagascar Basin through the fractures in the in the Southwest Indian Ridge (Warren, 1978) and flows further north along the deep western boundary of Madagascar (Warren, 1981). In the present investigation relatively lower temperature and salinity found at 4100*m* depth (49°S) which is consistent with the above hypothesis. However, the strong thermohaline fronts appeared near the Southwest Indian Ridge suggests the blockage of further northward movement of AABW eventhough minor fractures in the ridge may allow the penetration of the bottom water (Warren, 1978). In the present investigation we did not find any signature of the AABW further northwards beyond 49°S latitude.

3.4 Heat content variability and its implications

The meridional heat transport has a significant role in the global climate system. Eddies are one of the principal mechanisms which are responsible for the meridional heat

transfer (Peterson et al., 1984; Pillsbury and Bottero, 1984). Since there is a predominant variation in temperature in the frontal region, fronts are potential regions for higher heat flux. Thus the variation in heat content of the upper ocean from western to eastern region of the southern sector of the Indian Ocean is essential for a comprehensive understanding of the global climatic changes.

The air sea interaction processes depends on the heat content of the upper ocean. Heat content in the frontal zone is affected by the mixed layer developed due to convergence of two watermasses. The latitudinal distributions of heat content in the upper 500 *m* along the two meridional sections are depicted on Fig. 13. The heat-content changes indicate the different regimes of water masses and sharp boundaries between them. The meridional variations in the heat content facilitate the study of the poleward transport of oceanic heat. A dramatic change of 989 $\times 10^7$ J/m^2 in the heat content at ~42°S is encountered across the merged frontal region occupied by ARF and STF along 45°E. A change in the meridional gradient between 48°S to 52°S demarcates the Subantarctic and Antarctic zones to the north and south of it. An undulation in the profile of heat content from 35 to 40°S indicates the dynamic instability due to the eddy or mesoscale activities (see Plate 3 in Huges and Ash, 2001). The formation of heat transferring eddies have been observed near the well defined oceanic fronts in southern ocean (Joyce and Patterson, 1977). Along the meridional section 57°30'E, an abrupt change of 1405 $\times$ 10^7 J/m^2 in the heat content at ~44°S highlights the strength of merged ARF and STF (Fig. 13). The generation of frontal eddies is responsible for the faster meridional heat transfer and the formation of such eddies are common at the subtropical frontal region (Lutjeharms and Valentine, 1988).

A rapid fall of heat content at 57°30'E is observed slightly southward compared to 45°E. We note that a similar southward shift was also observed in the position of the merged ARF and STF (Fig. 3). One of our significant findings reveals that western part of the study region carries more heat content (Fig.13), compared to the eastern section. The meridional drop in heat content computed for a distance of 55km at 42°S along 45°E was 44% whereas, at 44°S along 57°30'E it was 58%, which may disclose the strength

of the merged ARF + STF towards east in the present study region. The dynamic nature of the merged ARF and STF may cause eddy shedding which would enhance a poleward heat transfer. The Subtropical convergence which is the northern boundary of the southern ocean exhibits a higher degree of horizontal variability in the heat content which promotes a faster meridional transport of heat from subtropics to polar region. Hence, we suggest that the observed variation of heat content influence the meridional heat transfer which is crucial for the studies related to global climatic variability.

4. Conclusions

This study investigates the latitudinal extent of the circumpolar fronts, merged ARF+STF, SAF and PF in the Indian Ocean sector of the Southern Ocean along 45° and 57°30'E sections, where earlier observations are limited. ARF+STF was observed between 40°15' and 42°15'S along 45°E whereas, it was shifted to more southwards (between 43°50'S and 45°40'S) along 57°30'E. Further, SAF was tapering from ~4° to 1.5° latitude width along 45°E and 57°30'E sections respectively. The results of the present study show a larger southward shift in the position of ARF+STF by 2° latitude compared to earlier investigations. The PF was identified between 48°S and 52°S with a width of ~4° latitude along 45°E. Thermocline was completely absent south of 50°S as a result of additional vertical mixing caused by winds, apart from the density mixing. A remarkable increase in MLT is seen from 45° to 52°S concomitant with the wind enhancement. A significant correlation between the MLT, WW depth and wind speed was noticed from 49° to 56°S which disclose that wind speed is the major reason for mixing in the upper layers and the variation of WW depth in the polar region. The present study exhibited also the presents of important watermasses like STSW, SASW, Mode Water, AAIW, CDW and AABW along the 45°E meridional section covering from 30°S to polar region. The poleward heat transfer may be enhanced by the eddy shedding due to merged ARF and STF. Since the poleward transport of heat from subtropics was predominantly promoted by the higher degree of horizontal variability in the heat content between the subtropics and polar region, perhaps this is the major cause for the global climatic changes.

ACKNOWLEDGMENTS

The authors thank Dr. H. K. Gupta, Secretary, Dept. of Ocean Development for the help in implementing the **Pilot Expedition to Southern Ocean** and Dr. R. Sanjeeva Rao, Dept. of Science & Technology, New Delhi for the financing the XBT probes. Help rendered in the implementation and completion of this study by cruise participants and staff at NCAOR is acknowledged.

References

Bathen, H.K., 1971. Heat storage and advection in the northern Pacific Ocean. Journal of Geophysical Research 76, 676 – 687.

Belkin, I. M., Gordon, A. L., 1996. Southern Ocean fronts from the Greenwich Meridian to Tasmania. Journal of Geophysical Research 101, 3675 – 3696.

Blintoff, N.L., McDougall., 1999. Decadal changes along an Indian Ocean section at 32°S and their interpretation. Journal of Physical Oceanography 30, 1207-1222.

CSIRO Cookbook for Quality Control of Expendable Bathythermography (XBT) Data, 1993. CSIRO, Australia, p. 74.

Deacon, G. E. R., 1937. The hydrology of the Southern Ocean. Discovery Reports 15, 3-122.

Fine, R.A., 1993. Circulation of Antarctic Intermediate Water in the South Indian Ocean. Deep Sea Research 40, 2021 – 2042.

Fu, L. L., 1986. Mass, heat and fresh water fluxes in the South Indian Ocean. Journal of Physical Oceanography 16, 1683-1693.

Gordon, A. L., 2003. The brawniest retroflection. Nature 42 (27), 904- 905.

Harris, T.F.W., 1972. Sources of the Agulhas Current in the spring of 1964, Deep Sea Research 19, 633-650.

Holliday, N. P., Read, J. F., 1998. Surface oceanic fronts between Africa and Antarctica. Deep Sea Research I 45, 217-238.

Huges, C. W., Ash, E.R., 2001. Eddy forcing of the mean flow in the Southern Ocean, Journal of Geophysical Research 106, 2713-2722.

Joyce, T.M., Patterson, S.L., 1977. Cyclonic ring formation at the polar front in the Drake Passage. Nature 265(5590), 131-133.

Lutjeharms, J. R. E., Valentine, H. R., 1984. Southern ocean thermal fronts south of Africa. Deep Sea Research I, 31, 1461-1475.

Lutjeharms, J. R. E., 1985. Location of frontal systems between Africa and Antarctica: some preliminary results. Deep Sea Research I, 32, 1499-1509.

Lutjeharms, J. R. E., Valentine, H. R., 1988. Eddies at subtropical convergence south of Africa. Journal Physical Oceanography 31, 1461-1475.

McCartney, M.S., 1977. Subantarctic Mode Water. In: Angel, M.V. (Ed.), A voyage of Discovery. Pergamon, New York, pp. 103-119

McCartney, M.S., 1982. The subtropical recirculation of Mode Waters. Journal of Marine Research 40 supplementary, 427-464.

Menon, H. B., RameshBabu, V., Sastry, J. S., 1988. Apparent Relationship between thermal regime in Antarctic waters and Indian summer monsoon. Indian Journal of Marine Sciences 17, 87-90.

Molinelli, E.J., 1981. The Antarctic influence on Antarctic Intermediate Water. Journal of Marine Research 39, 267 – 293.

Nagata, Y., Michida., Y., Umimura, Y., 1988. Variation of position and structures of the oceanic fronts in the Indian Ocean sector of the Southern Ocean in the period from 1965 to 1987. In: Sahrhage, D. (Ed.), Antarctic Ocean and Resources Variability. Springer, New York, pp 92-98.

Nowlin, W. D. Jr., Klinck, J. M., 1986. The physics of the Antarctic Circumpolar Current. Review Geophysics 24, 469-491.

Orsi, A.H., Whitworth III, T., Nowlin, W. D. Jr., 1993. On the circulation and stratification of the Weddell Gyre. Deep Sea Research I 40, 169-203.

Orsi, A.H. Whitworth, III, T., Nowlin, Jr, W.D., 1995. On the meridional extent and fronts of the Antarctic Circumpolar Current. Deep Sea Research I 42, 641-673.

Park, Y.–H., Gamberoni, L., Charriaud., E., 1993. Frontal structure, water masses and circulation in the Crozet Basin. Journal of Geophysical Research 98, 12361 – 12385.

Park, Y.–H., Charriaud, E., Fieux, M., 1998. Thermohaline structure of Antarctic surface water/winter water in the Indian sector of the Southern Ocean. Journal of Marine Systems 17**,** 5-23.

Peterson, R.G., Nowlin, W.D.Jr., Whitworth, T. III., 1984. Generation and evolution of a cyclonic ring at Drake Passage in early 1979. Journal of Physical Oceanography 12, 712-719.

Peterson, R.G., Whitworth, T. III., 1989. The Subantarctic and Polar Fronts in relation to deep water masses through the Southwestern Atlantic. Journal of Geophysical Research 94, 10,817-10,838.

Pillsbury, R.D., Bottero, J.S., 1984. Observations of currents rings in the Antarctic zone at Drake Passage. Journal of marine Research 42, 853-872.

Read, J.F., Pollard, R.T., 1993. Structure and transport of Antarctic Circumpolar Current and Agulhas Return Current at 40°E. Journal of Geophysical Research 98, 12281-12295.

Reid, J.L., 2003. On the total geostrophic circulation of the Indian Ocean : flow patterns, tracers and transports. Progress in Oceanography 56, 137-186.

Ridgway, K.R., 1995. An application of a new depth correction formula to archived XBT data. Deep Sea Research I, 42(8), 1513-1519.

Rintoul, S.R., Donguy, J.R., Roemmich, D.H., 1997. Seasonal evaluation of upper ocean thermal structure between Tasmania and Antarctica. Deep Sea Research I 44, 1185-1202.

Rintoul, S.R., Bullister, J.L., 1999. A late winter hydrographic section from Tasmania to Antarctica. Deep Sea Research I 46, 1417-1454.

Rintoul, S. R., Sokolov, S., 2001. Baroclinic transport variability of the Antarctic Circumpolar Current south of the Australia (WOCE repeat section SR3). Journal of Geophysical Research 106, 2815 – 2832.

Rintoul, S.R., Sokolov, S., Church, J., 2002. A 6-year record of baroclinic transport variability of the Antarctic Circumpolar Current at 140 degrees E derived from expendable bathythermograph and altimeter measurements. Journal of Geophysical Research-Oceans 107 (C10), Art. No. 3155 SEP-OCT.

Sokolov, S., Rintoul, S.R., 2002. Structure of Southern Ocean Fronts at 140°E. Journal of Marine Systems 37(1-3), 151-184.

Sparrow, M.D., Heywood, K.J., Brown, J., Stevens D.P., 1996. Current structure of the South Indian Ocean. Journal of Geophysical Research 101 (C3), 6377 – 6391.

Stramma, L., Lutjeharms, J.R.E., 1997. The flow field of the subtropical gyre of the South Indian Ocean. Journal of Geophysical Research 102 (C3), 5513 – 5530.

Thadathil, P., Saran, A.K., Gopalakrishna, V.V., Vethamony, P., Araligidad, N., 2002. XBT fall rate in waters of extreme temperature: a case study in Antarctic Ocean. Journal of Atmospheric and Ocean Technology 19**,** 391-396.

Toole, J.M., Warren, B.A., 1993. A hydrographic section across the subtropical South Indian Ocean. Deep Sea Research 40, 1973-2019

Warren, B.A. 1978. Bottom water transport through the Southwest Indian Ridge. Deep Sea Research 25, 315-321.

Warren, B.A. 1981. Trans-Indian hydrographic section at lat, 18°S: property distribution and circulation in the South Indian Ocean. Deep Sea Research 28, 759-788.

Xiaojun, Y., Martinson, D.G., Dong, Z., 2004. Upper-ocean thermal structure and its temporal variability in the southeast Indian Ocean. Deep Sea Research I 51, 333-347.

Legend to Table

Table – 1 Adopted property indicators for identification of fronts

Legend to Figures

Fig. 1 XBT (●) and CTD (Δ) station locations superimposed on bathymetry (shaded). Section along 45°E and 57°30' were occupied during 29 January~17 February and 22~29 February, 2004, respectively.

Fig. 2 Vertical structure of temperature **(a)** along 45°E and **(b)** along 57°30'E.

Fig. 3 Vertical structure of salinity **(a)** along 45°E and **(b)** along 57°30'E

Fig. 4 Vertical temperature profiles from XBT observations along 45°E between **(a)** 31 and 39°S, **(b)** 41 and 44°S, and **(c)** 46 and 56°S. The inset show the same profiles with constant range of temperature (-2 to 28°C) to facilitate a comparison. The ordinate and abscissa represent depth (*m*) and temperature (^{o}C), respectively.

Fig. 5 Meridional variation of (a) mixed layer thickness (*m*) and (b) wind speed (ms^{-1}), along 45°E. The thick line represents a polynomial fit to the data.

Fig. 6 Meridional variation of (a) Winter Water depth (*m*) and (b) Winter Water Temperature (°*C*), along 45°E. The thick line represents a polynomial fit to the data.

Fig. 7 Vertical structure of potential temperature (°C) with bottom topography

Fig. 8 Vertical structure of salinity (‰) with bottom topography

Fig. 9 Vertical structure of density with bottom topography

Fig.10 TS diagram **a)** from 32 to 36°S and **b)** from 37 to 40°S *

Fig. 11 TS diagram **a)** from 41 to 44°S and **b)** from 45 to 48°S

Fig. 12 TS diagram **a)** from 49 to 52°S and **b)** from 53 to 56°S

Fig. 13 Meridional variation of heat content integrated for 0-500*m* water column along 45°E (solid line) and 57°30'E (dashed line).

* psu – practical salinity unit (‰)

Table – 1: Adopted property indicators for identification of fronts

Frontal structure	Adopted criterion		
	Temperature (°C)	**Salinity (‰)**	**Reference**
Agulhas Return Front (ARF)	19~17°C at surface; 10°C isotherm from 300 to 800m	35.54~35.39 ‰ at surface; 35.57~34.90‰ at 200m	Holliday and Read (1998); Belkin and Gordon (1996); Sparrow *et al*.(1996)
Subtropical Front (STF)	17~10.6°C at surface; 12~10°C at 100m	35.35~34.05‰ at surface; 35~34.6‰ at 100m; 34.92~34.42‰ at 200m	Holliday and Read (1998); Belkin and Gordon (1996); Sparrow *et al*.(1996)
Subantarctic Front (SAF)	9.7~6.3°C at surface; 8~5°C at 200m	34.0~33.85‰ at surface; 34.40~34.11‰ at 200m	Holliday and Read (1998); Belkin and Gordon (1996); Sparrow *et al.* (1996); Park *et al*. (1993)
Polar Front (SPF)	5.5~2.7°C; northern limit of the 2°C isotherm below 200m	33.8~33.9‰ at surface	Holliday and Read (1998); Belkin and Gordon (1996); Sparrow et al.(1996)

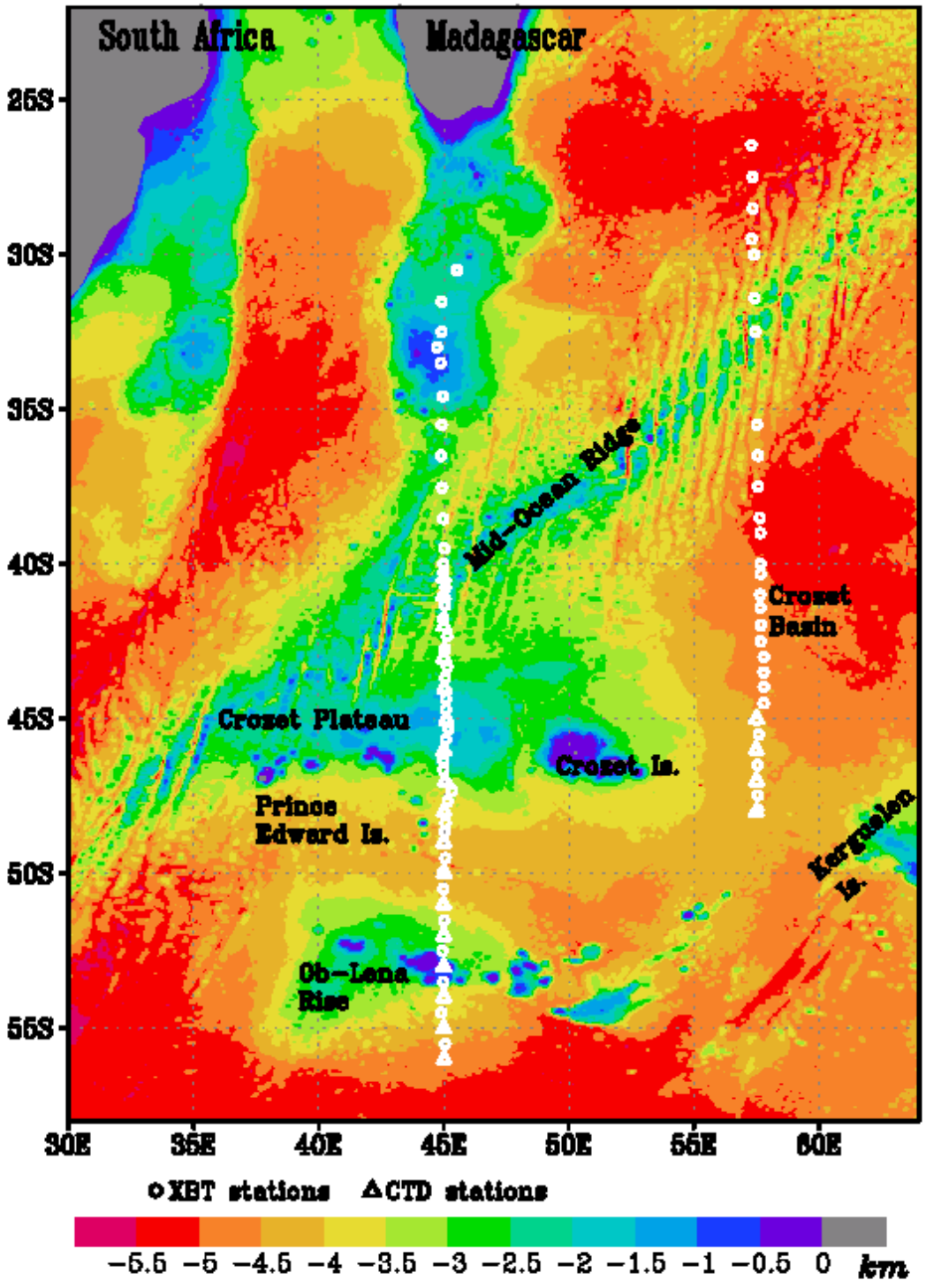
South Africa
Madagascar
25S
30S
35S
40S
45S
50S
55S
30E
35E
40E
45E
50E
55E
60E
Mid-Ocean Ridge
Crozet Basin
Crozet Plateau
Crozet Is.
Prince Edward Is.
Kerguelen Is.
Ob-Lena Rise
XBT stations
CTD stations
−5.5 −5 −4.5 −4 −3.5 −3 −2.5 −2 −1.5 −1 −0.5 0
km

Fig. 1

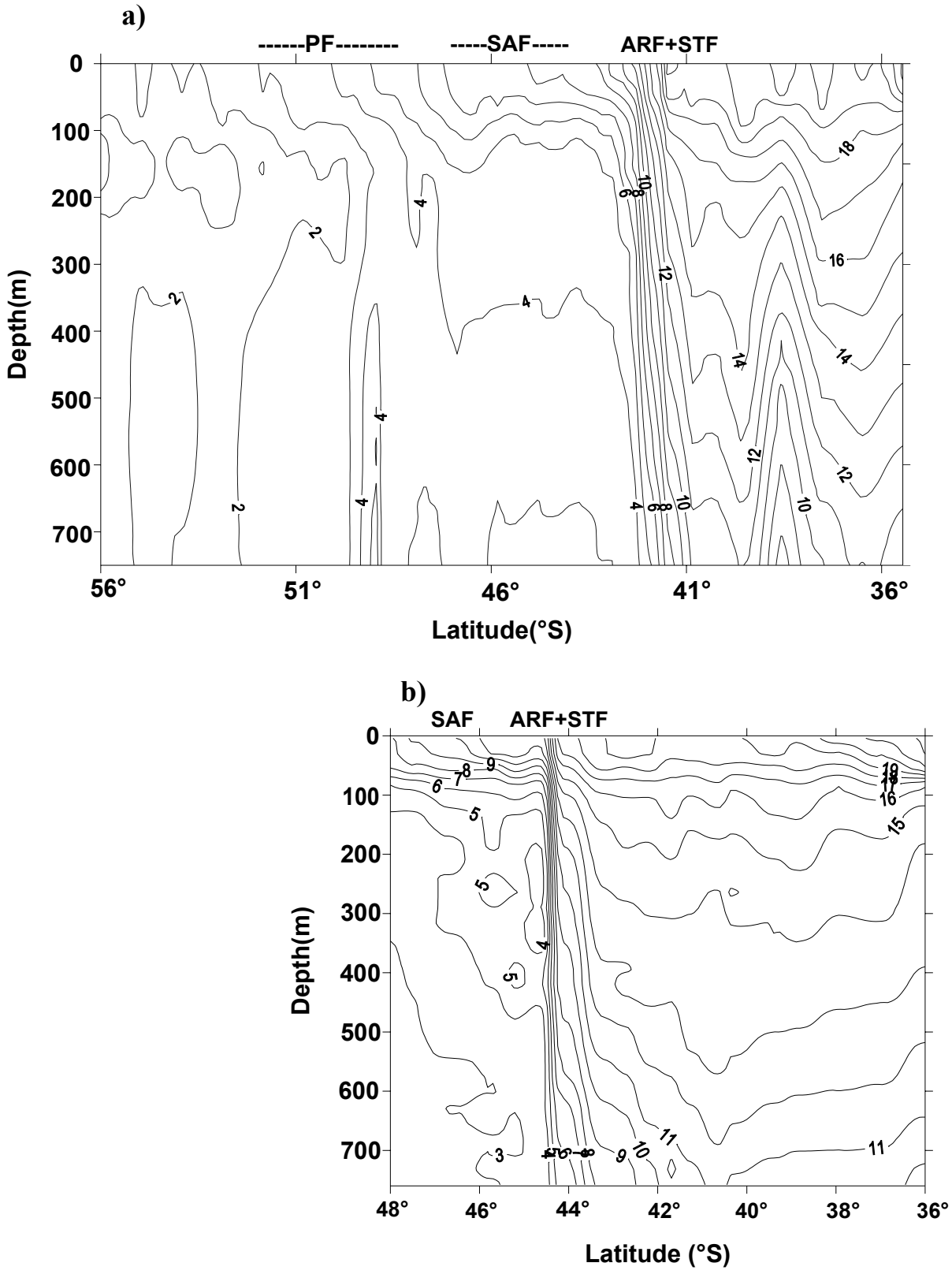
a)
------PF--------
-----SAF-----
ARF+STF
Depth(m)
Latitude(°S)
b)
SAF
ARF+STF
Depth(m)
Latitude (°S)

Fig. 2

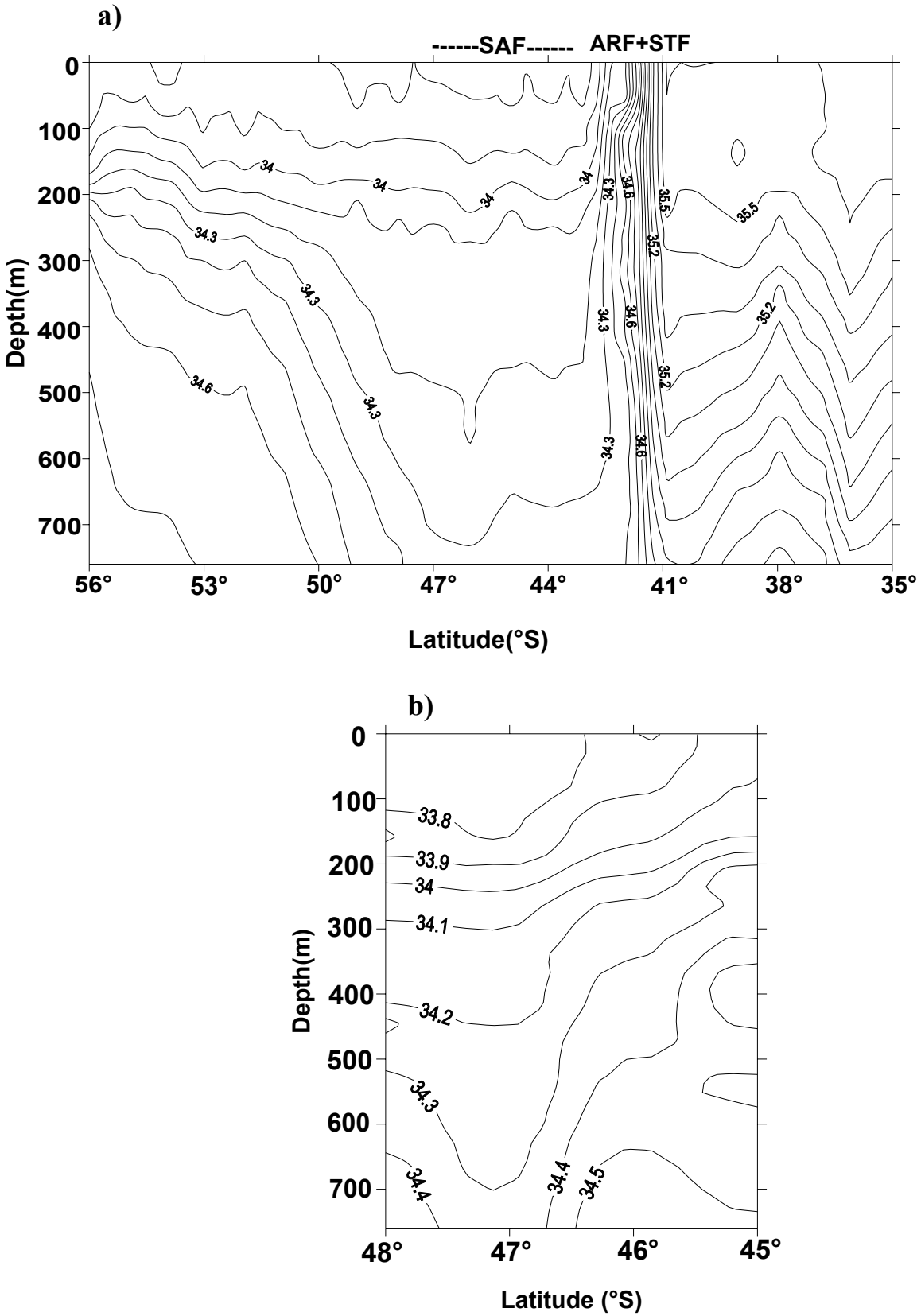
a)
------SAF------ ARF+STF
Depth(m)
Latitude(°S)
56°
53°
50°
47°
44°
41°
38°
35°
b)
Depth(m)
Latitude (°S)
48°
47°
46°
45°

Fig. 3

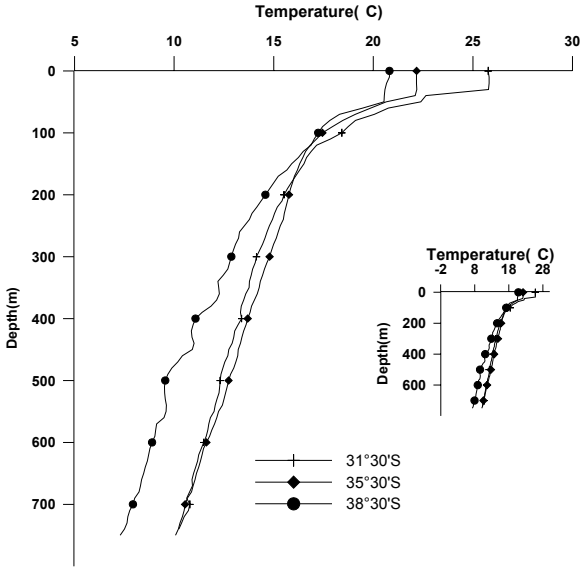
Temperature(C)
5
10
15
20
25
30
0
100
200
300
400
500
600
700
Depth(m)
Temperature(C)
-2
8
18
28
0
200
400
600
Depth(m)
31°30'S
35°30'S
38°30'S

a.

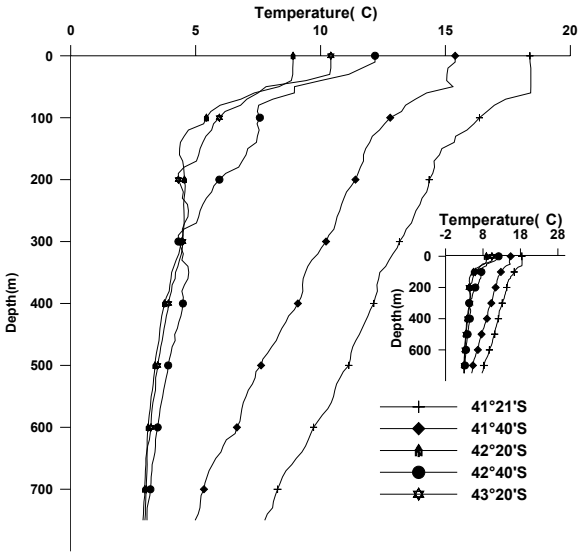
Temperature(C)
0
5
10
15
20
0
100
200
300
400
500
600
700
Depth(m)
Temperature(C)
-2
8
18
28
0
200
400
600
Depth(m)
41°21'S
41°40'S
42°20'S
42°40'S
43°20'S

b.

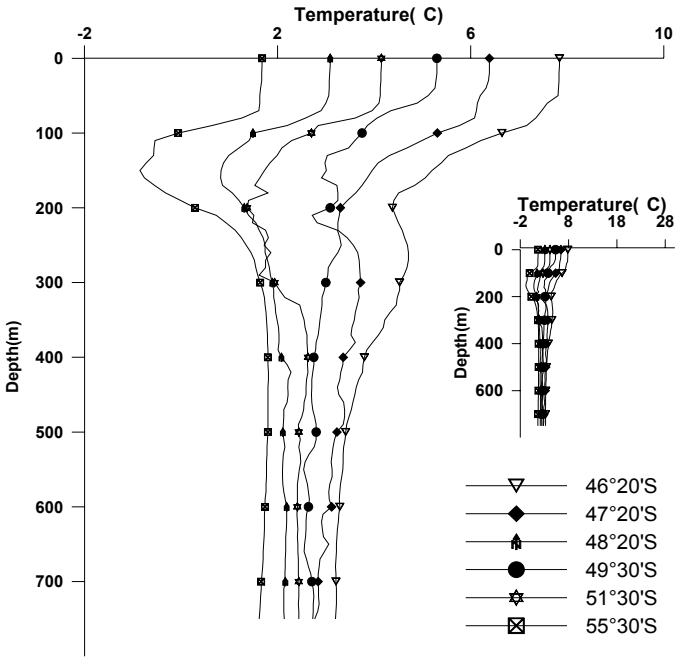
Temperature(C)
-2
2
6
10
0
100
200
300
400
500
600
700
Depth(m)
Temperature(C)
-2
8
18
28
0
200
400
600
Depth(m)
46°20'S
47°20'S
48°20'S
49°30'S
51°30'S
55°30'S

c.

Fig. 4

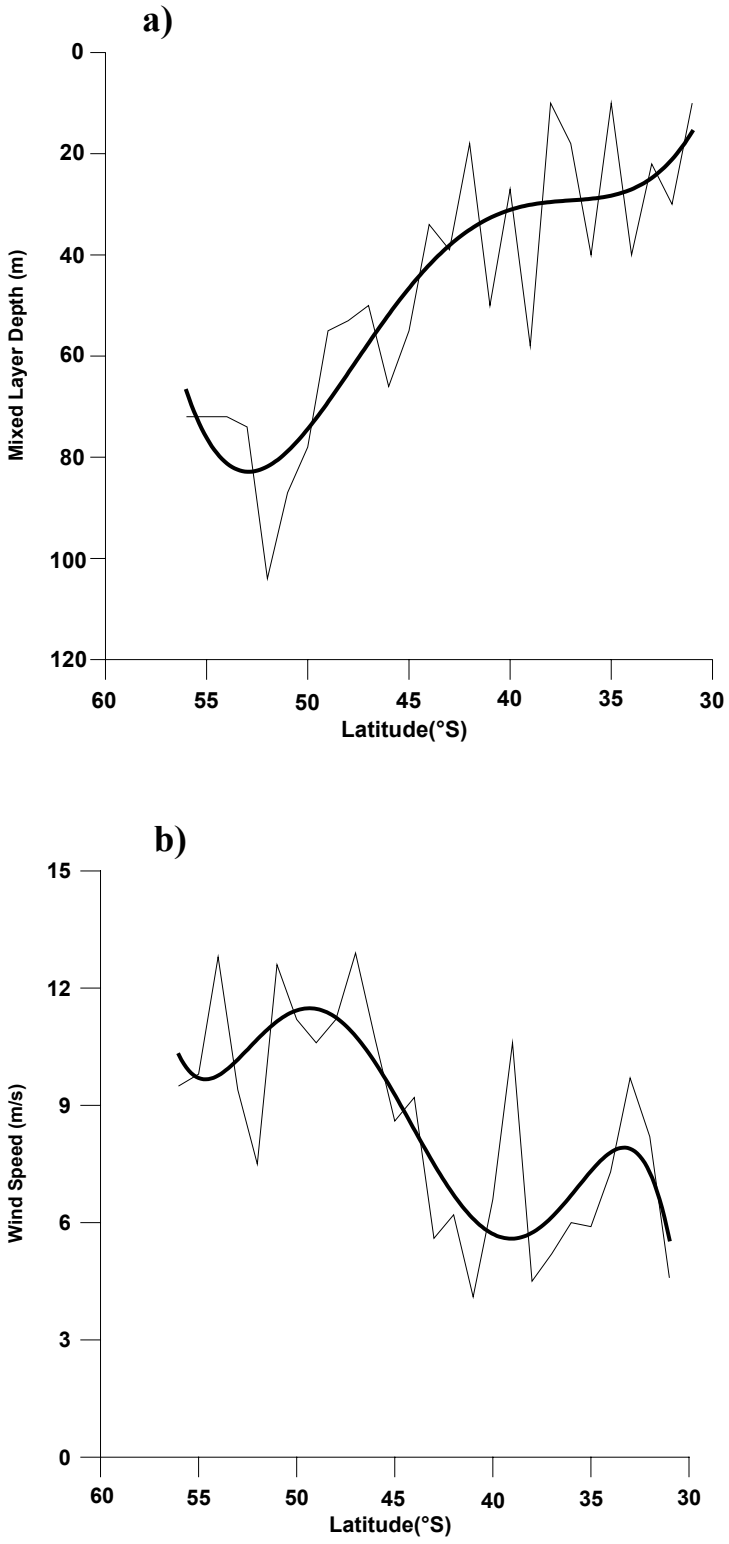
a)
0
20
40
60
80
100
120
Mixed Layer Depth (m)
60
55
50
45
40
35
30
Latitude(°S)
b)
15
12
9
6
3
0
Wind Speed (m/s)
60
55
50
45
40
35
30
Latitude(°S)

Fig. 5

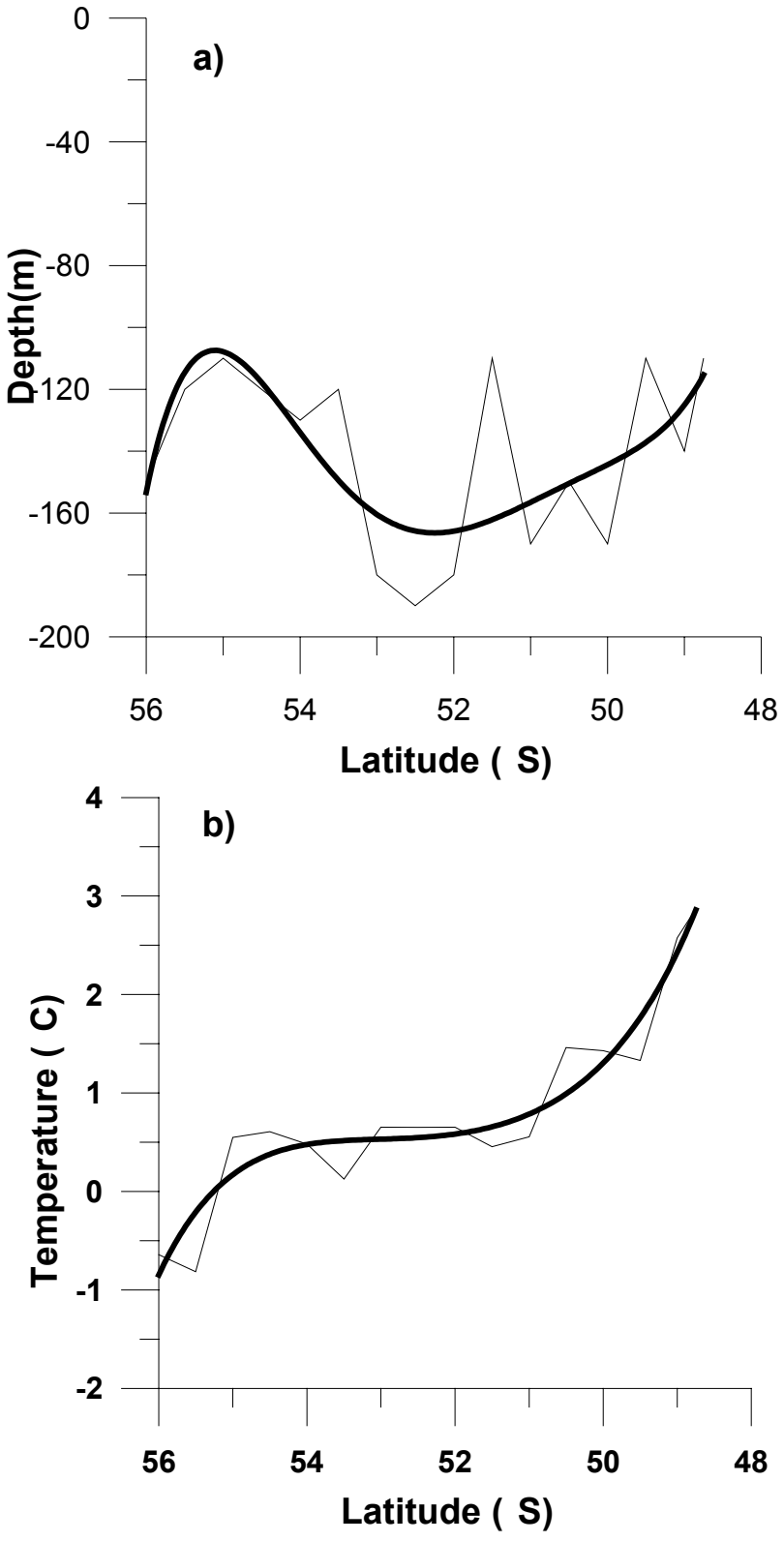
a)
0
-40
-80
-120
-160
-200
Depth(m)
56
54
52
50
48
Latitude (S)
b)
4
3
2
1
0
-1
-2
Temperature (C)
56
54
52
50
48
Latitude (S)

Fig. 6

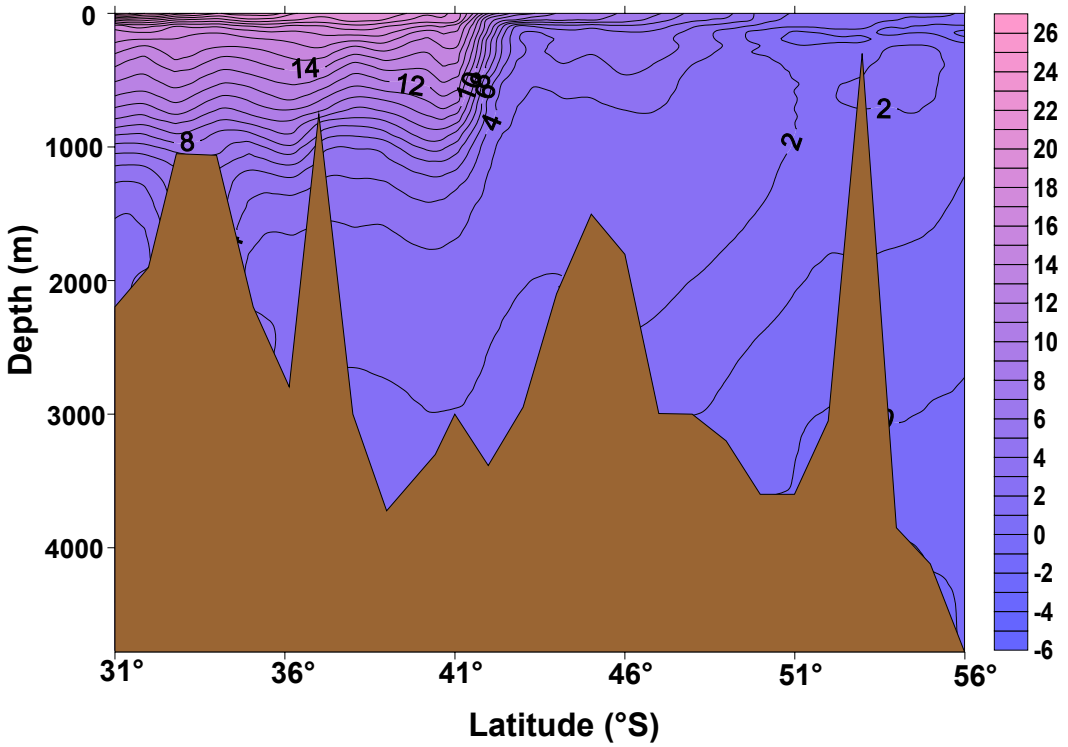
Depth (m)
0
1000
2000
3000
4000
31°
36°
41°
46°
51°
56°
Latitude (°S)
14
12
8
4
2
2
8
26
24
22
20
18
16
14
12
10
8
6
4
2
0
-2
-4
-6

Fig. 7

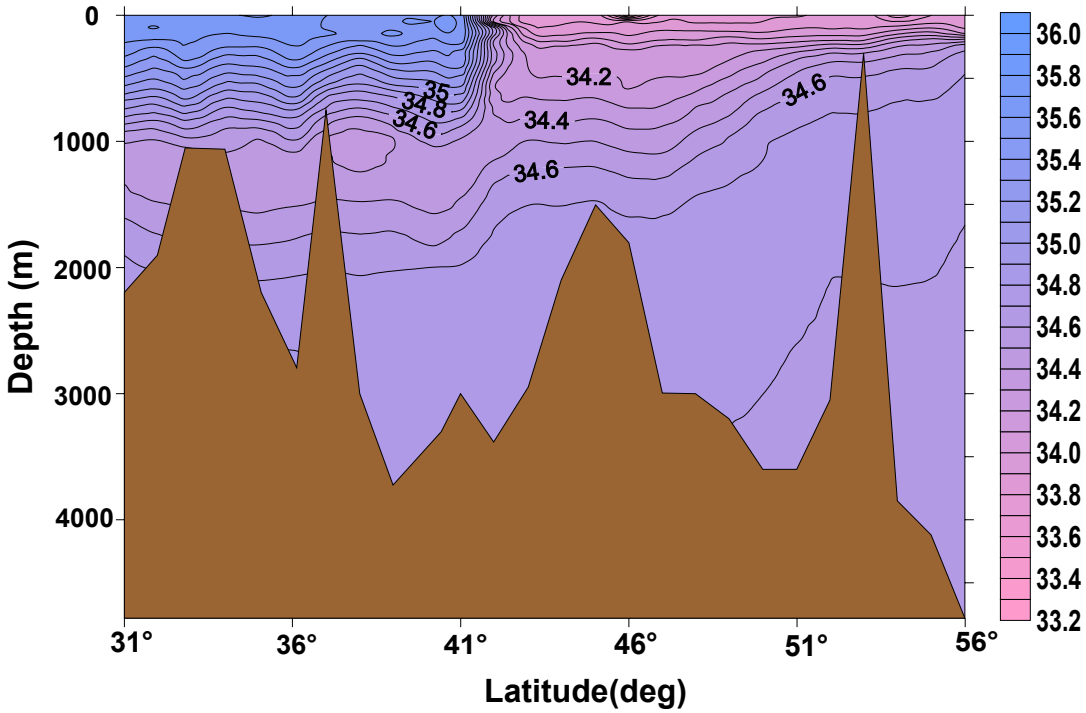
Depth (m)
0
1000
2000
3000
4000
31°
36°
41°
46°
51°
56°
Latitude(deg)
35
34.8
34.6
34.2
34.4
34.6
34.6
36.0
35.8
35.6
35.4
35.2
35.0
34.8
34.6
34.4
34.2
34.0
33.8
33.6
33.4
33.2

Fig. 8

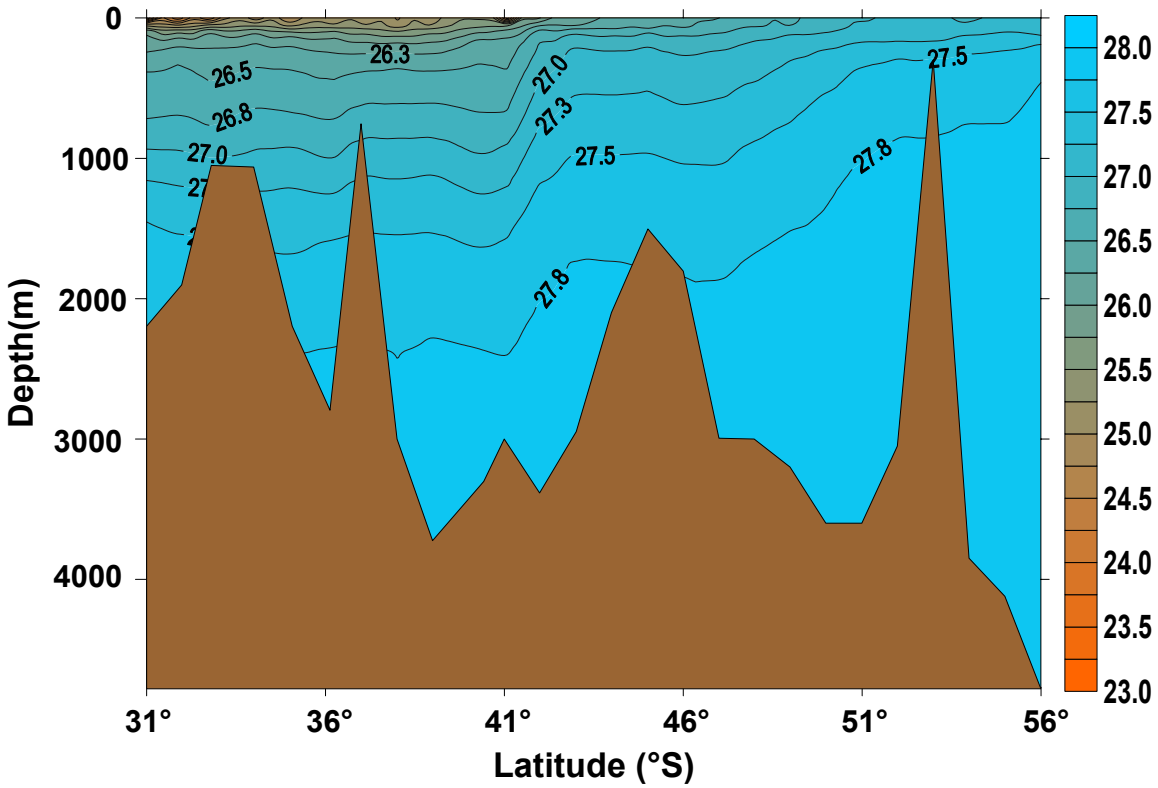
0
1000
2000
3000
4000
Depth(m)
31°
36°
41°
46°
51°
56°
Latitude (°S)
26.3
26.5
26.8
27.0
27.0
27.3
27.5
27.5
27.8
27.8
28.0
27.5
27.0
26.5
26.0
25.5
25.0
24.5
24.0
23.5
23.0

Fig. 9

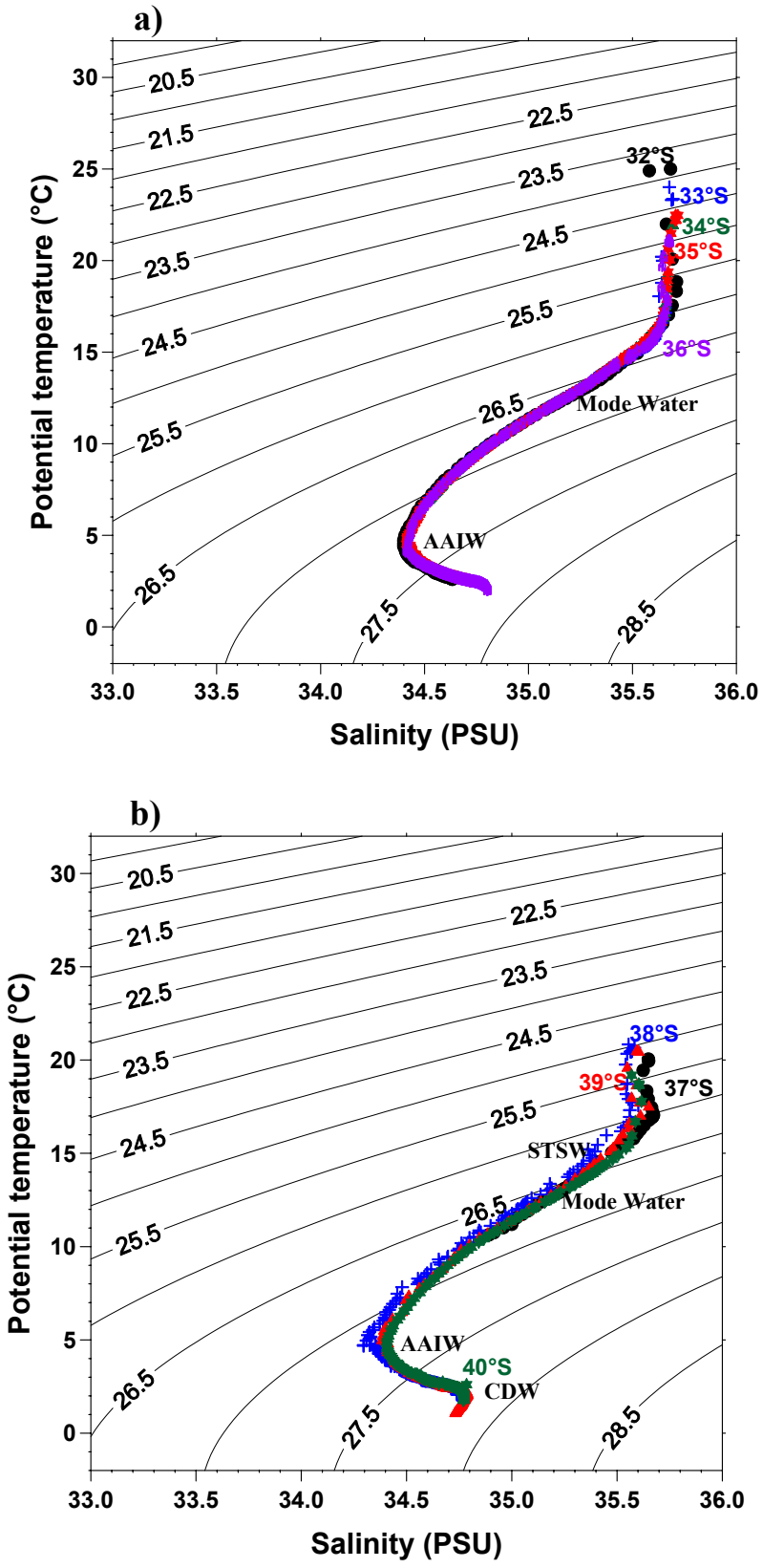
a)
Potential temperature (°C)
Salinity (PSU)
20.5
21.5
22.5
23.5
24.5
25.5
26.5
27.5
28.5
32°S
33°S
34°S
35°S
36°S
Mode Water
AAIW
b)
Potential temperature (°C)
Salinity (PSU)
38°S
39°S
37°S
STSW
Mode Water
AAIW
40°S
CDW

Fig. 10

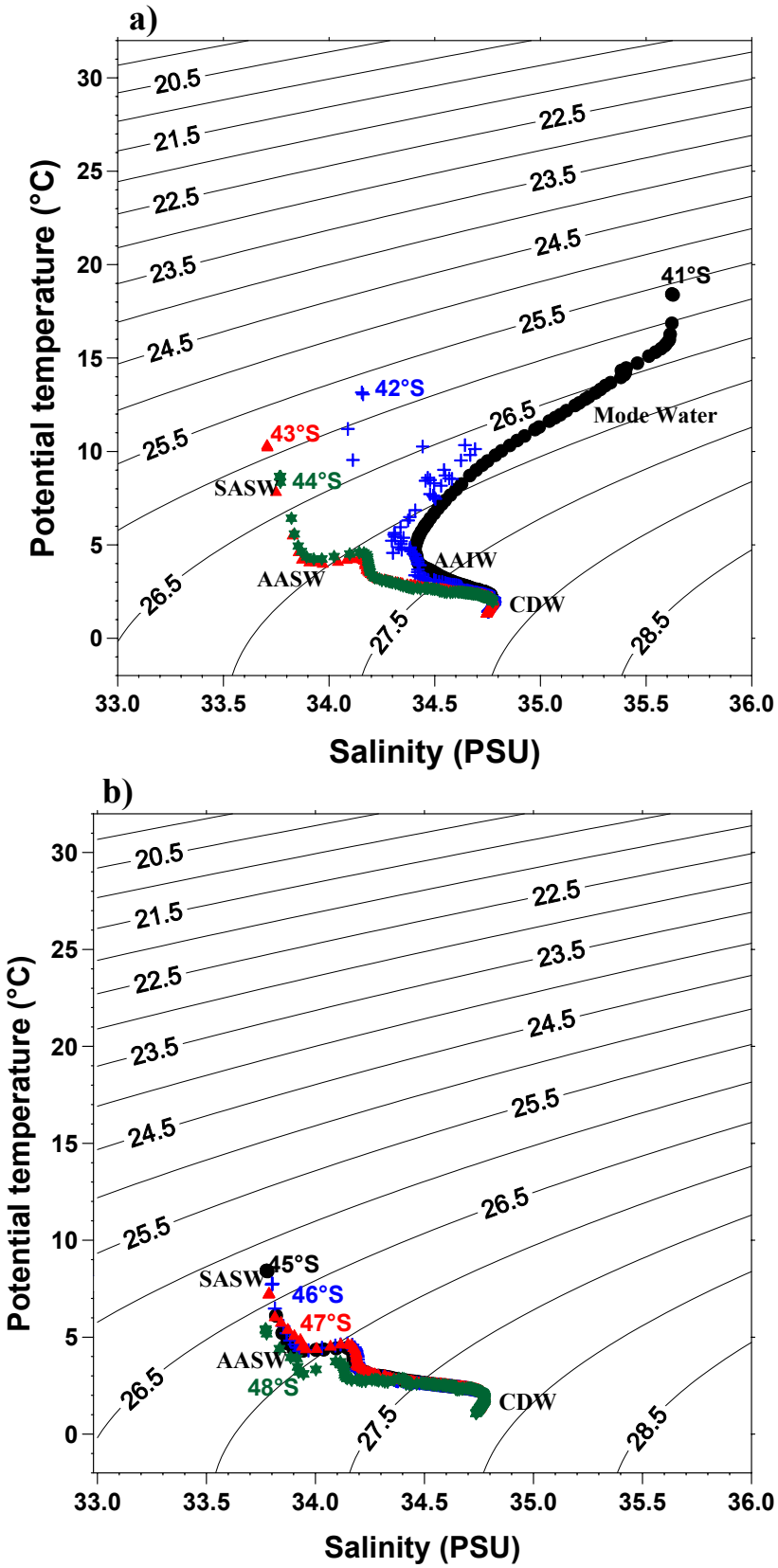
a)
Potential temperature (°C)
Salinity (PSU)
20.5
21.5
22.5
23.5
24.5
25.5
26.5
27.5
28.5
41°S
42°S
43°S
44°S
SASW
AASW
AAIW
CDW
Mode Water
b)
Potential temperature (°C)
Salinity (PSU)
45°S
46°S
47°S
48°S
SASW
AASW
CDW

Fig. 11

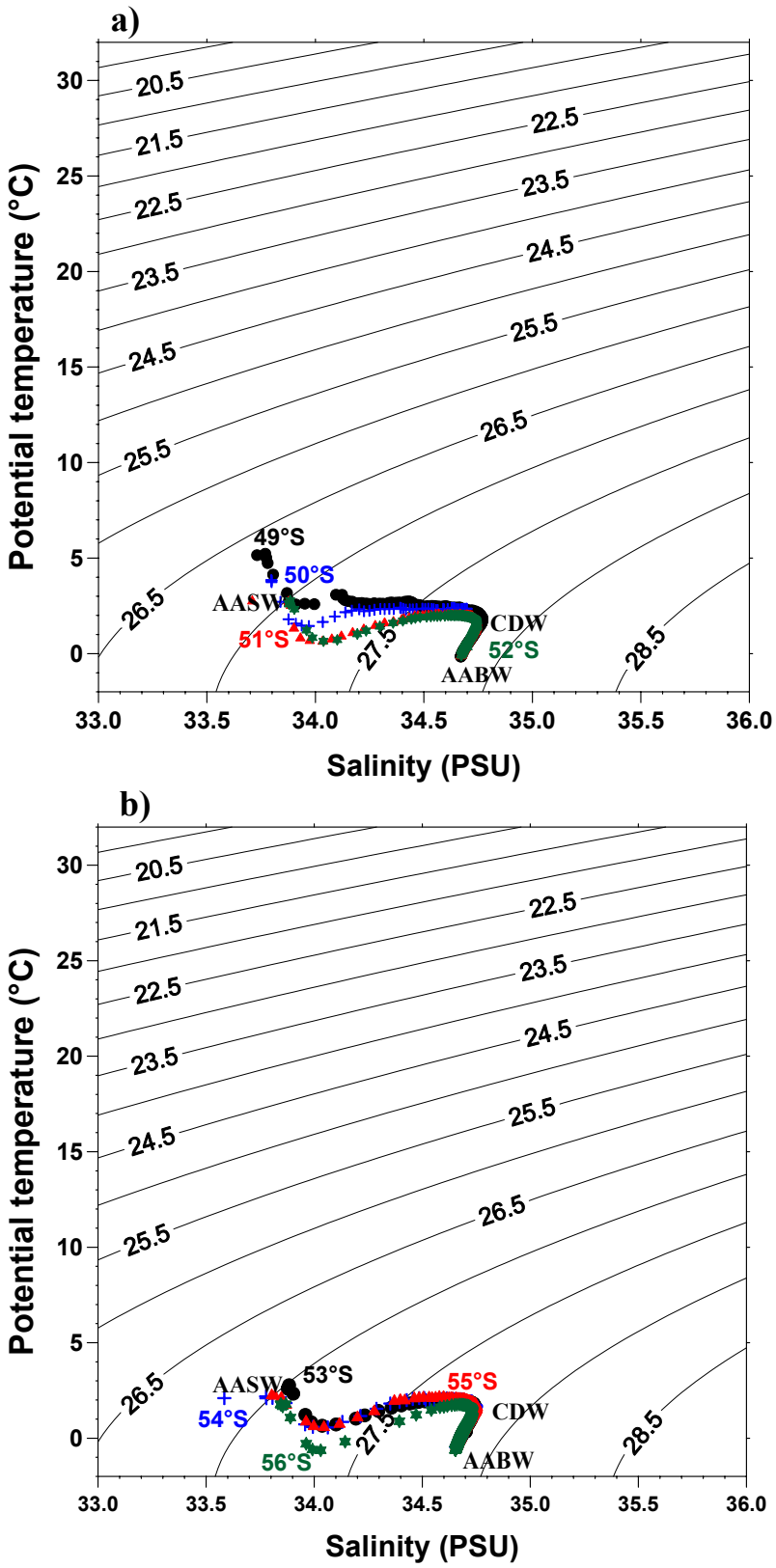
a)
Potential temperature (°C)
Salinity (PSU)
20.5
21.5
22.5
23.5
24.5
25.5
26.5
27.5
28.5
49°S
50°S
AASW
CDW
51°S
52°S
AABW
b)
Potential temperature (°C)
Salinity (PSU)
AASW
53°S
54°S
55°S
CDW
56°S
AABW

Fig. 12

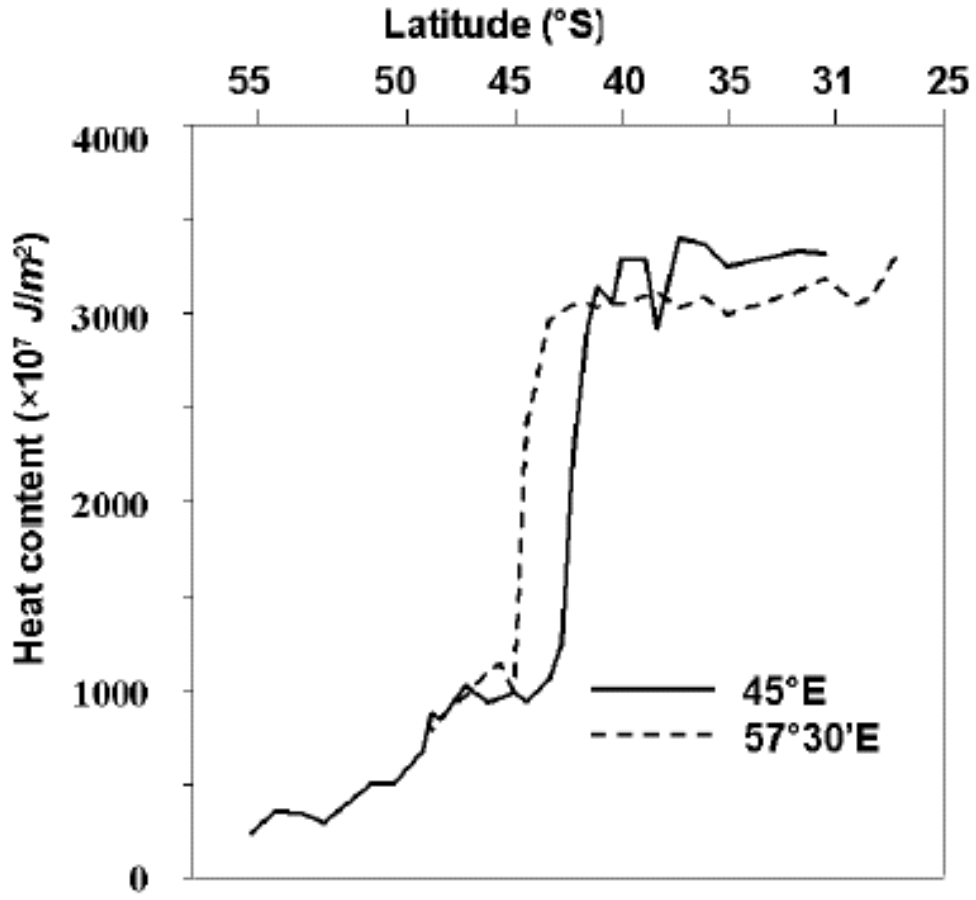
Latitude (°S)
55
50
45
40
35
31
25
4000
3000
2000
1000
0
Heat content (×10⁷ J/m²)
45°E
57°30'E

Fig. 13